Jing-Fung LIN[1], Cong-Hui HUANG[2], Tzong-Shyng LEU[3]

Dep. Computer Application Engineering, Far East University (1), Dep. of Automation and Control Engineering, Far East University (2), Dep. of Aero- and Astronautics Engineering, Cheng Kung University (3)

Measurement of Retardance and Birefringence in PLZT10/30/70 Film with PLT Layer

Abstract. *Lanthanum-modified lead zirconate titanate (PLZT10/30/70) with and without seeding layer of (PLT10/0/100) were successfully deposited on glass substrate via a sol-gel process, and planar electrodes of TaAl were formed on the films by sputtering. The thickness of PLZT and PLT layer were 500nm and 24nm, respectively. The retardance of PLZT film was measured by a heterodyne interferometer and enhanced by application of PLT layer. The birefringence of PLZT10/30/70 films with and without PLT10/0/100 layer were determined to be 0.11 and 0.088, respectively, larger than 0.006 for PLZT9/65/35 with PLT9/0/100 layer in the literature. The average transmittance of PLZT film with PLT layer was 80.3%, a little smaller than that of PLZT film without PLT layer of around 86.5%. Results imply that PLT layer plays a key role in the increase of retardance, leading to a higher birefringence, and avoids optical loss.*

Streszczenie:** Zmodyfikowaną lantanem ceramikę ołów-cyrkon-tytan (PLZT10/30/70) z i bez warstwy PLT10/0/100 nałożono na podłoże szklane metodą sol-gel a płaskie elektrody TaAl uformowano na powłoce przez napylanie. Grubości warstw PLZT i PLT były odpowiednio 500nm i 24nm. Pokrycie powłoki PLZT zmierzono za pomocą spektrometru heterodynowego i wzmocniono przez zastosowanie warstwy PLT. Dwójłomność powłok PLZT10/30/70 z i bez warstwy PLT10/0/100 wyznaczono odpowiednio jako 0,11 i 0,088, wartości większe niż, podawana w literaturze, 0,006 dla PLZT9/65/35 z warstwą PLT9/0/100. Średnia transmitancja powłoki PLZT z warstwą PLT była 80,3%, trochę mniejsza niż około 86,5% dla PLZT bez PLT. Z badań wynika, że warstwa PLT gra kluczową rolę we wzroście pokrycia prowadzącego do większej dwójłomności i zmniejsza straty optyczne.* ***Pomiar pokrycia i dwójłomności powłoki PLZT10/30/70 z warstwą PLT

Keywords: *Birefringence, PLZT, Retardance, Sol-Gel.*
Słowa kluczowe: Dwójłomność, PLZT, Pokrycie, Metoda sol-gel

Introduction

One of the ferroelectric thin films as lanthanum-modified lead zirconate titanate (PLZT) ceramics is renowned optical ceramics materials with great multi-functional properties, such as piezoelectricity, pyroelectricity, and electro-optical (EO) effects. PLZT is used in EO applications because of their excellent EO performance, rapid response, and high optic transmittance in the visible wavelength spectrum [1, 2]. Since the discovery of PLZT ceramics with high optical transparency and good EO characteristics in 1970's, extensive studies have concerned on these materials.

Recently, increasing interest has been shown in the fabrication of thin films for electronic and optical deviceswitches, spatial light modulators, electro-optical modulators [3-5], and light shutter [6]. In particular, a thin-film-type device made of PLZT materials is required for large area devices and also for integration with other processes. High phase retardation (retardance) is mandatory for all EO applications, especially in the case of certain devices such as optic shutters, for which it constitutes the most critical property.

To achieve such high phase retardation, either the film needs to be quite thick or an effective electrode configuration is adopted [1]. Previous investigations have revealed that a high and uniform electric field was applied to the films when an embedded-electrodes structure was used [5, 6]. A PLZT9/65/35 film with a PLT9/0/100 seeding layer applied to the glass and the embedded electrode structure showed a high retardance. The birefringence value was obtained 0.0054 ~ 0.006 for the films thickness of 1, 2, and 4μm, respectively [1].

PLZT thin films with various compositions have been extensively investigated during the last decades. The reported PLZT thin films were prepared by various methods. They include radio-frequency sputtering [7, 8], pulsed laser deposition [9, 10] (PLD), electron beam deposition [11] (EBD), chemical vapor deposition [12] (CVD) and sol-gel processing [13-15]. Among these methods, sol–gel is well accepted to be a promising method in the preparation of ferroelectric thin films because it offers several advantages over the others. These advantages include (a) higher deposition rates, (b) good stoichiometry control, (c) larger area, pinhole-free film deposition and (d) lower initial facility costs and lower processing temperature [16].

In this paper, the seeding layer of $(Pb_{0.9}La_{0.1})TiO_3$ (PLT10/0/100) was prepared on glass substrate and then $(Pb_{0.9}La_{0.1})(Zr_{0.3}Ti_{0.7})_{0.975}O_3$ (PLZT10/30/70) was deposited on the PLT layer. In addition, planar electrodes of TaAl were formed on the PLZT film by sputtering. The principal axis of the PLZT sample was characterized by a developed EO modulated circular heterodyne interferometer [17] and the retardance was further characterized by a previously developed linear heterodyne interferometer [18]. To the best of our knowledge and compared to other measurement systems, the interferometer [17, 18] we used has the advantages as it is stable, high dynamic range, less influenced by the environments. For the completeness, we described the linear heterodyne interferometer [18] in next section and make comparisons with PLZT7/30/70 with and without a PT layer under transverse electric field in optical and surface properties [18].

Experimental methodology

The stock solutions were prepared corresponding to the general formula $(Pb_{0.9}La_{0.1})(Zr_{0.3}Ti_{0.7})_{0.975}O_3$ by means of a methanol-based sol-gel method. Reagent grade lead acetate trihydrate $(Pb(CH_3COO)_2{\cdot}3H_2O)$, lanthanum acetate hydrate $(La(CH_3COO)_3{\cdot}6H_2O)$, titanium isopropoxide $(Ti((CH_3)_2CHO)_4)$, and zirconium n-propoxide $(Zr(OC_3H_7)_4)$ were used as the starting materials. The starting materials were dissolved separately in methanol in combination with achelation agents ($C_5H_8O_2$ and C_2H_7NO) to form four types of pre-solutions (i.e., Pb, La, Zr, and Ti pre-solutions). For PLT precursor, Pb, La, and Ti pre-solutions were mixed and stirred for one hour. On the other hand, Pb, La, Zr, and Ti pre-solutions were mixed according to the molar ratio of 13.31/1/3.80/7.67 and stirred for one hour to prepare PLZT precursor. We use excess Pb acetate to consider the loss during the process.

First of all, the PLZT precursors were coated onto a glass substrate using a spin coater at (1) 300rpm for 5s and 2000rpm for 35s. (2) 400rpm for 5s and 1000rpm for 35s. The above steps were repeated five times to increase the thickness of PLZT film with 0.5μm (procedure (1) was repeated three times and procedure (2) was done two times). The films were baked on a hot plate at 100℃ for 5min between each layer deposition. After deposition of PLZT films, the films were placed directly into a hot furnace at a temperature of 500℃ for 30min. To prepare the PLZT10/30/70 films with a PLT10/0/100 layer, the PLT precursor was coated onto a glass substrate which was used as a seeding layer by using a spin coater (Chemat Technology Inc., KW-4A) at (1) 500rpm for 5s. (2) 1500rpm for 35s. The PLT film with thickness of 24nm was baked at 100℃ for 5min and then the PLT film was placed directly into a hot furnace at a temperature of 500℃. The rise rate of temperature is 500℃/30min. Afterwards, the PLZT precursors were coated onto PLT layer according to the same method as above-mentioned to obtain samples of PLZT films with a PLT seeding layer. In order to measure the retardance of PLZT films, planar electrodes of TaAl by 3mm spacing were formed on the films by sputtering. The choice of one of Al alloy films as TaAl is that it has low electricity resistivity and the sputtering equipment is available.

The optical configuration [18] for measuring the electric-field-induced retardance of PLZT10/30/70 film in the study is shown in Fig. 1. The configuration in Fig. 1 is based on the common-path linear heterodyne interferometer. In Fig. 1, a He–Ne laser light beam of wavelength 632.8 nm passes initially through a polarizer, and then through an EO modulator which is regulated by a saw-tooth waveform signal supplied by a function generator. Subsequently, the light beam passes through the sample, and finally an analyzer. The output light intensity is then detected by a photodetector. The final signal in Fig. 1 is processed by a lock-in amplifier in phase-lock for extracting the retardance in the sample. It is noted that the fast axis angle is firstly determined by a developed circular heterodyne interferometer [17] also using a phase-lock technique and the axis of sample is rotated to 22.5°.

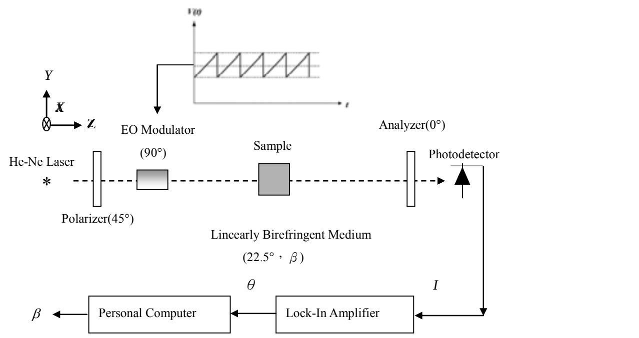

Fig.1. Schematic illustration of an electro-optic linear heterodyne interferometer for the retardance measurement

According to the Jones matrix formalism, the vector of the electric field emerging from the analyzer in the optical configuration shown in Fig. 1 has the form as [18]

(1)
$$E = A(0^\circ).S(22.5^\circ,\beta).EO(90^\circ,\omega t).P(45^\circ).E_{in}$$
$$= \begin{bmatrix} 1 & 0 \\ 0 & 0 \end{bmatrix} \begin{bmatrix} \cos(\frac{\beta}{2}) + i\frac{\sqrt{2}}{2}\sin(\frac{\beta}{2}) & i\frac{\sqrt{2}}{2}\sin(\frac{\beta}{2}) \\ i\frac{\sqrt{2}}{2}\sin(\frac{\beta}{2}) & \cos(\frac{\beta}{2}) - i\frac{\sqrt{2}}{2}\sin(\frac{\beta}{2}) \end{bmatrix}$$
$$\begin{bmatrix} e^{-i\frac{\omega t}{2}} & 0 \\ 0 & e^{i\frac{\omega t}{2}} \end{bmatrix} \begin{bmatrix} \frac{1}{2} & \frac{1}{2} \\ \frac{1}{2} & \frac{1}{2} \end{bmatrix} \begin{bmatrix} 0 \\ E_0 \end{bmatrix} e^{i\omega_0 t},$$

where E_0 is the amplitude of the incident field, $A(0^\circ)$ represents the Jones matrix of the analyzer parallel to the x-axis, $S(22.5^\circ,\beta)$ represents the Jones matrix of the sample, and β is the phase retardation (retardance) of the sample. Furthermore, $EO(90^\circ,\omega t)$ represents the Jones matrix of the EO modulator driven by a saw-tooth voltage waveform at a frequency ω and with its fast axis parallel to the y-axis, and $P(45^\circ)$ represents the Jones matrix of the polarizer set at 45° to the x-axis.

As a result, the intensity of the transmitted light, I, can be expressed as

(2)
$$I = E_0^2 \times (2 + (1-\cos(\beta))\cos(\omega t) - \sqrt{2}\sin(\beta)\sin(\omega t))/8$$
$$= I_{dc} + R\cos(\omega t - \theta),$$

where $I_{dc} = E_0^2/4$ is the dc component of the output light intensity , and E_0^2 is the intensity of the input light. The notation *R* represents $I_{dc}\sqrt{(1-\cos(\beta))^2 + (-\sqrt{2}\sin(\beta))^2}/2$, and *θ* represents $\tan^{-1}(-\sqrt{2}\sin(\beta)/1-\cos(\beta))$. Therefore, the retardance of the linearly birefringent medium can be determined by the phase-lock technique as Eq. (3).

(3) $\beta = 2\tan^{-1}(-\sqrt{2}/\tan\theta).$

Further, the surface roughness of PLZT films with and without a PLT seeding layer, respectively, were measured by an atomic force microscopy (AFM, Veeco-DI, AutoProbe CPR-II, AP-0100, America). The transmittances of PLZT films with and without a PLT seeding layer were performed by a conventional Ultraviolet-visible (UV-Vis) spectrophotometer (HELIOS OMEGA UV-Vis, Thermo Scientific, USA).

Results and discussions

After conducting the calibration and fine-tuning procedures, we perform a series of experiments. The first experiment in Fig. 1 is conducted to measure the retardance of a quarter-wave plate (Casix Inc., QWP0-633-04-4-R10) with nominal retardance of 90°. As shown in Fig. 2, the average retardance in the quarter-wave plate after a total of 10 measurements is determined to be 89.632°. The average relative error is just 0.41%, and these results validate the retardance measurement methodology.

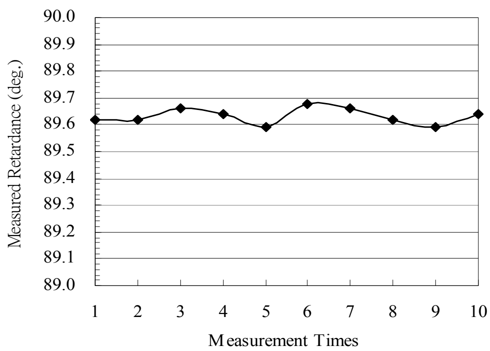

Fig.2. Measured retardance of the linearly birefringent medium (quarter-wave plate)

Secondly, the PLZT10/30/70 samples with and without a PLT10/0/100 seeding layer are prepared. The retardance properties of the PLZT samples with and without a PLT seeding layer are measured as the principal axis angle of 22.5° using the optical setup in Fig. 1. The application of direct-current voltage on the PLZT films is from 0V to 0.5V

(0V to 0.14V in increments of 0.02V, 0.19V and 0.21V are included). From the experimental results of PLZT without a PLT layer shown in Fig. 3, the maximum retardance is found to be 26.21° when the applied voltage is 0.12V. Accordingly, the PLZT with a PLT layer, the experimental results indicate that the maximum retardance is found to be 32.67° when the applied voltage is 0.13V. This is almost 6.5° larger than that in PLZT film without a PLT layer.

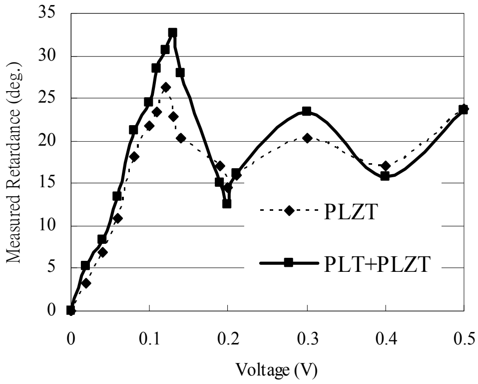

Fig.3. Absolute retardance of PLZT and PLZT with PLT

Subsequently, the birefringence Δn is determined by the wavelength λ, the retardance β and the optical path length L (thickness of flim) according to the formula as Eq. (4). Among them, the refractive index and the thickness of PLZT film are determined by a reflection Ellipsometer and known as 2.4 and 510nm, respectively. The thickness value is close to that of the SEM measurement (500nm).

(4) $\Delta n = \beta\lambda / 2\pi L,$

According to the measured retardance, using Eq. (4), the birefringence of PLZT10/30/70 films with and without a PLT10/0/100 layer can be determined to be 0.11 and 0.088, respectively. The results are larger than the birefringence about 0.0054 ~ 0.006 for PLZT9/65/35 with a PLT9/0/100 layer [1] and larger than the birefringence of about 0.001 ~ 0.004 for the PLZT epitxial films, which was investigated as a function of lanthanum content [19]. Simultaneously, the birefringence results are close to that of $LiNbO_3$ [19] single crystal (0.084).

We investigated the effect of the PLT10/0/100 layer on the surface morphology of the PLZT10/30/70 film by using AFM, as shown in Fig. 4. The AFM is used to investigate the surface roughness of PLZT films with and without a PLT layer in an area of 2μm x 2μm, respectively. The roughness of the film surface is expressed by the root-mean-square value. As shown in Fig. 4, the roughness of PLZT film with a PLT layer (4.01nm) is larger than that of PLZT film without a PLT layer (2.87nm) by almost 1 nm. Shin [20] et al. indicated the crystallinity of PLZT films increases with introduction of a PLT seeding layer because the lattice parameters of the PLT layer are matched well with those of PLZT. However, the larger roughness of PLZT with a PLT layer might be due to the stress or thermal mismatch between layers.

The optical transmittance spectra of the PLZT10/30/70 films with wavelength change are shown in Fig. 5, where interference oscillations were caused by the film structure. In addition to the reference spectra of glass substrate 91.4% illustrated in Fig. 5, the transmittance spectra of the PLZT10/30/70 films with and without a PLT10/0/100 seeding layer were presented. From the comparisons, the average transmittance of the PLZT film with a PLT seeding layer is 80.3% from 400 to 700nm (that is, in visible region), which is a little smaller than that of the PLZT film without a PLT seeding layer (86.5%). Hence the PLT seeding layer plays a key role in the increase of retardance (birefringence) and avoids optical loss for the addition of a PLT layer into PLZT film.

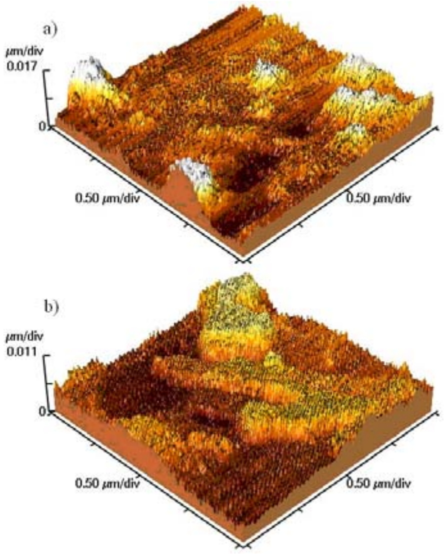

Fig.4. AFM surface images of (a) PLZT, (b) PLZT with a PLT layer

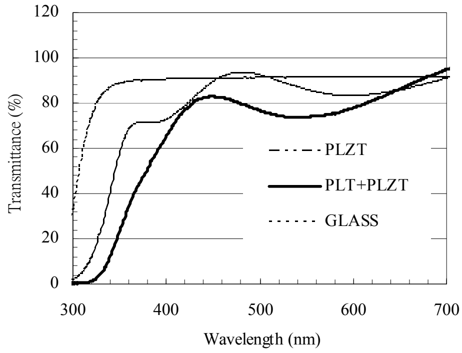

Fig.5. Optical transmittance spectra of glass substrate and the PLZT films

Compared to the previous study for PLZT7/30/70 film with a PT seeding layer [18], the forward and backward electrodes are composed of a sol-gel derived SnO_2 conductive layer and ITO, respectively. The measured birefringence and optical transmission of PLZT7/30/70 with a PT seeding layer are 0.0048, and 77.01%, respectively, are lower than those of PLZT10/30/70 film with a PLT10/0/100 seeding layer obtained in this study. Hence, the different composition, electrode type, and seeding layer play a key role in the EO performance of PLZT films. Further, the lattice parameters of the PLT layer are better matched with those of the PLZT than those of the PT or PbO layer [20] with the PLZT. Further. The increase of La amount in PLZT composition can improve the transmission is validated experimentally.

Conclusions

PLZT10/30/70 ferroelectric films with and without a PLT10/0/100 seeding layer were grown on glass substrate using a sol-gel method, and planar electrodes of TaAl by 3mm spacing were formed on the PLZT films using sputtering method. Further, the retardance is successfully measured by a previously developed electro-optical modulated linear heterodyne interferometer. Experimental results show that the birefringence of PLZT film with a PLT layer was determined to be 0.11. In addition, the surface roughness of PLZT with a PLT layer increases when compared with PLZT film without a PLT layer. At the same time, the transmittance of PLZT film with a PLT layer is 80.3%, which is a little smaller than that of PLZT film without introduction of PLT seeding layer (86.5%). Therefore, the retardance (birefringence), surface roughness, and optical transmittance of PLZT film can be varied by adding a PLT seeding layer, which is suitable for the high retardance application. In the future, we hope to study the effects of the thickness of the seeding layer, gap of electrodes, and the annealing temperature, respectively, on the increase of retardance and birefringence.

Acknowledgments

This work was supported in part by NSCT under Grant No. 100-2221-E-269-012.

REFERENCES

[1] Choi J.J., Kim D.Y., Park G.T., Kim H.E., Effect of electrode configuration on phase retardation of PLZT films grown on glass substrate, *Journal of the American Ceramic Society*, 87 (2004), 950-952
[2] Haertling G.H., Land C.E., Hot-pressed $(Pb,La)(Zr,La)O_3$ ferroelectric ceramics for electrooptic applications, *Journal of the American Ceramic Society*, 54 (1971), 1-11
[3] Preston K.D., Haertling G.H., Comparison of electro-optic lead-lanthanum zirconate titanate films on crystalline and glass substrate, *Applied Physics Letters*, 60 (1972), 2831-2833
[4] Baude P.F., Ye C., Tamagawa T., Polla. D.L., Fabrication of sol-gel derived ferroelectric $Pb_{0.865}La_{0.09}Zr_{0.65}Ti_{0.35}O_3$ optical waveguides, *Journal of Applied Physics*, 73 (1993), 7960-7962
[5] Title M.A., Lee S.H., Modeling and characterization of embedded electrode performance in transverse electro-optic modulators, *Applied Optics*, 29 (1990), 85-98
[6] Taniguchi Y., Murakami K., Kobayashi H., Tanaka S., A $(Pb,La)(Zr,Ti)O_3$ (PLZT) polarization-plane rotator with a buried electrode structure for a midinfrared electro-optical shutter, *Japan Journal of Applied Physics*, 36 (1997), 2709-2714
[7] Ishida M., Matsunami H., Tanaka T., Preparation and properties of ferroelectric PLZT thin films by rf sputtering, *Journal of Applied Physics*, 48 (1977), 951-953
[8] Adachi H., Mitsuyu T., Yamazaki O., Wasa K., Ferroelectric $(Pb,La)(Zr,Ti)O_3$ epitaxial thin films on sapphire grown by rf planar magnetron sputtering, *Journal of Applied Physics*, 60 (1986), 736-741
[9] Cheng H.F., Spectroscopic characteristics of $Pb_{0.95}La_{0.05}(Zr1-yTiy)_{0.9875}O_3$ plasma and growth behavior of thin films by pulsed laser deposition, *Journal of Applied Physics*, 78 (1995), 4633-4639
[10] Yeh M.H., Liu K.S., Ling Y.C., Wang J.P., Lin I.N., The growth behavior of $Pb_{0.95}La_{0.05}(Zr1-yTiy)_{0.9875}O_3$ films on silicon substrates synthesized by pulsed laser deposition, *Journal of Applied Physics*, 77 (1995), 5335-5340
[11] Panda B., Ray S.K., Dhar A., Sarkar A., Bhattacharya D., Chopra K.L., Electron S.K., beam deposited lead-lanthanum-zirconate-titanate thin films for silicon based device applications, *Journal of Applied Physics*, 9 (1996), 1008-1012
[12] Baude P.F., Ye C., Tamagawa T., Polla D.L., Fabrication of sol-gel derived ferroelectric optical waveguides, *Journal of Applied Physics*, 73 (1993), 7960-7962
[13] Choi H.W., Park Y.S., Dougherty J., Jang N.W., Park C.Y., Electrical and optical properties of PLZT thin films on ITO coated glass by sol-gel processing, *Journal of Material Science*, 35 (2000), 1475-1479
[14] Tokumitsu E., Nakamura R., Ishiwara H., Nonvolatile memory operations of metal–ferroelectric–insulator–semiconductor (MFIS) FET's using PLZT/STO/Si(100) structures, *IEEE Electron Device Letters*, 18 (1997), 160-162
[15] Li K.K., Wang F., Haertling G.H., Antiferroelectric lead zirconate thin films derived from acetate precursors, *Journal of Material Science*, 30 (1995), 1386
[16] Kong L.B., Ma J., Preparation and characterization of antiferroelectric PLZT2/95/5 thin films via a sol-gel process, *Journal of Materials and Letters*, 203 (2002), 638-642
[17] Lin J.F., Lo. Y.L., The new circular heterodyne interferometer with electro-optic modulation for measurement of the optical linear birefringence, *Optics Communications*, 260 (2006), 486-492
[18] Lin J.F., Jeng J.S., Chen W.R., Wu B.H., Measurement of optical and surface properties of PLZT thin films, *Optik*, 123 (2012), 276-279
[19] Kamehara N., Ishii M., Sato K., Kurihara K., Kondo M., Optical properties of epitaxial plzt thin films, *Journal of Electroceramics*, 21 (2008), 99-102
[20] Shin J.S., Lee W.J., Effects of seed layers on the characteristics of $(Pb,La)(Zr,Ti)O_3$ thin films prepared by electron cyclotron resonance plasma enhanced chemical vapor deposition, *Japan Journal of Applied Physics*, 36 (1997), 6909-6914

***Authors**: prof. Jing-Fung Lin, No.49, Zhonghua Rd., Xinshi Dist., Tainan City 74448, Taiwan, E-mail: jacklin@cc.feu.edu.tw; dr Cong-Hui Huang, No.49, Zhonghua Rd., Xinshi Dist., Tainan City 74448, Taiwan, E-mail: ch_huang@cc.feu.edu.tw; dr Tzong-Shyng Leu, No.1, Ta-Hsueh Rd., Tainan 70101, Taiwan, E-mail: tsleu@mail.ncku.edu.tw.*